Spiro[3.3]heptane as a Non-collinear Benzene Bioisostere

Kateryna Prysiazhniuk,[a] Oleksandr P. Datsenko,[a] Oleksandr Polishchuk,[a] Stanislav Shulha,[a] Oleh Shablykin,[a,b] Liza Nikandrova,[c] Kateryna Horbatok,[c] Iryna Bodenchuk,[c] Petro Borysko,[c] Dmytro Shepilov,[c] Iryna Pishel,[c] Vladimir Kubyshkin,[a] Pavel K. Mykhailiuk[a]*

[a] Enamine Ltd., Winston Churchill Street78, 02094 Kyiv (Ukraine). E-mail: Pavel.Mykhailiuk@gmail.com
[b] V.P. Kukhar Institute of Bioorganic Chemistry and Petrochemistry NAS of Ukraine, 02094 Kyiv (Ukraine).
[c] Bienta, Winston Churchill Street 78, 02094 Kyiv (Ukraine).

Dedicated to the people of Ukraine

Abstract. Spiro[3.3]heptane can mimic the *mono*-, *meta*- and *para*-substituted phenyl rings in drugs.

Introduction. The phenyl ring is a key structural element in chemistry. It is the most popular ring in natural products, [1] bioactive compounds, and drugs.[2]

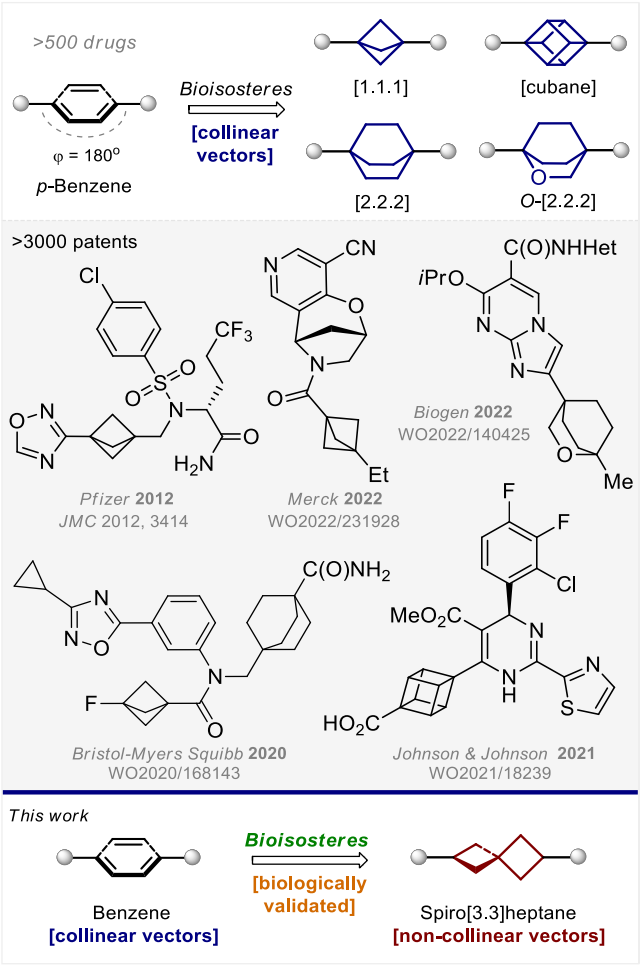

Scheme 1. Bicyclo[1.1.1]pentane, cubane, bicyclo[2.2.2]octane, and 2-oxabicyclo[2.2.2]octane as saturated bioisosteres of benzene. This work: spiro[3.3]heptane as a saturated bioisostere of benzene.

In 2012, *Stepan* and colleagues showed that a replacement of the central phenyl ring in a bioactive compound with the bicyclo[1.1.1]pentane improved physicochemical properties and retained bioactivity (Scheme 1).[3,4] Later, analogous studies were undertaken with cubane, [5,6] bicyclo[2.2.2]octane [7] and 2-oxabicyclo[2.2.2]octane. [8] During the past decade, these scaffolds proved to be useful in drug discovery, medicinal chemistry, and supramolecular chemistry as saturated benzene bioisosteres.[9] In the case of *para*-substituted benzene, all four bioisosteres retained the original collinearity of exit vectors (φ = 180º).

In this work, we have discovered that spiro[3.3]heptane with non-collinear exit vectors can mimic the *mono*-, *meta*- and *para*-substituted phenyl rings in drugs (Figure 1).

Results and discussion. ***Synthesis***. Spiro[3.3]heptane core is well known in the literature. It is often used in medicinal chemistry as a unique 3D-shaped scaffold.[10,11] However, to the best of our knowledge, it has never been used as a benzene bioisostere before.[12,13]

Substituted spiro[3.3]heptanes are usually synthesized using linear approaches: addition of ketenes to activated/strained alkenes;[14,15] alkylation of malonate esters;[16] rearrangements of cyclopropanes,[17] or other reactions.[18]

In a search for a modular approach to spiro[3.3]heptanes from the commercially available starting materials we focused our attention on the reaction between keteneiminium salts with alkenes into cyclobutanones. [19] Recently, this reaction was adjusted to prepare polycyclic [20] and *poly*-substituted spiro[3.3]heptanes.[21] We envisioned that this strategy could also be applied to make *mono*- and *di*-substituted spiro[3.3]heptanes (to mimic the corresponding *mono*- and *di*-substituted benzenes in bioactive compounds) without the additional (poly)substitution.

Indeed, the thermal reaction of the *N*,*N*-dimethylamide of cyclobutane carboxylic acid with various alkenes in the presence of $(CF_3SO_2)_2O$/collidine followed by hydrolysis of the intermediate vinamidinium salts efficiently gave spiro[3.3]heptanes **1**-**29** in good yields (Scheme 2). The reaction was compatible with active chlorine (**6**, **7**), and bromine (**8**, **9**, **11**, **12**) atoms; TMS (**13**, **15**), TBDMS (**14**), *N*-Ts (**17**, **18**) groups, and even with the azetidine ring (**17**). The reaction worked equally well for aliphatic (**1**-**18**) and aromatic (**19**-**29**) alkenes. Amides of substituted cyclobutane carboxylic acids gave the desired spiro[3.3]heptanes **30**-**39** as well.

The analogous reaction between *N*,*N*-dimethylacetamide (DMA), and the substituted cyclobutylidenes gave spiro[3.3]heptanes **40**-**42**. The reaction between *N*,*N*-dimethylisobutyramide and styrene led to the formation of product **43** (Scheme 2).

Important to note, that this method towards spiro[3.3]heptanes worked efficiently on milligram, gram, and even multigram scales (**2**, **15**, **40**). On a milligram-to-gram scale, we purified products by silica gel column chromatography. On a gram-to-multigram scale, we isolated the products by distillation under reduced pressure. The structure of products **18**, **24**, **30**, and **41** was confirmed with X-ray crystallographic analysis.[22]

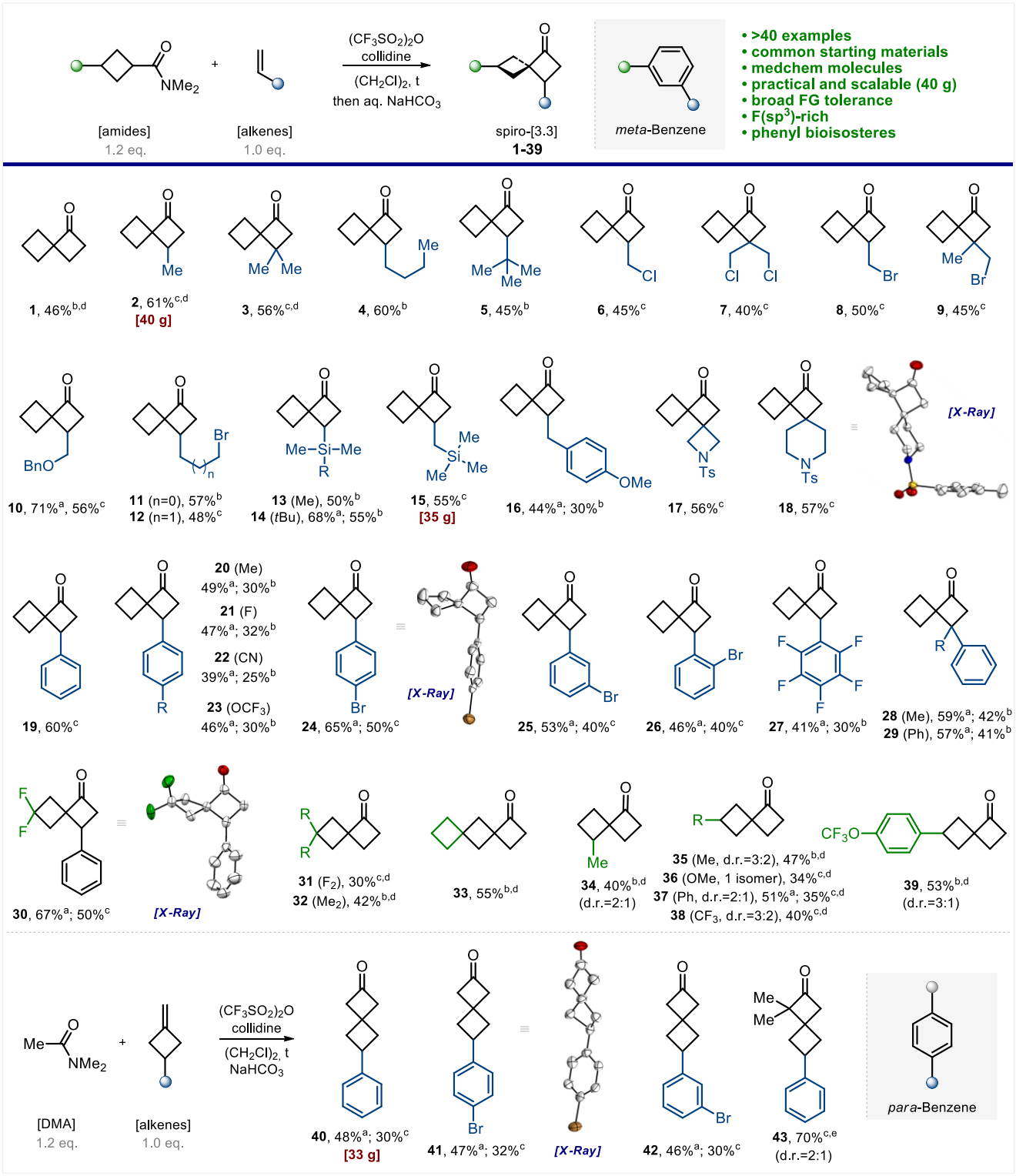

Scheme 2. Reaction conditions: (i) alkene (1 equiv.), amide (1 equiv.), triflic anhydride (1.2 equiv.), colliding or lutidine (1.2 equiv.), 1,2-dichloroethane, reflux, 16 h; (ii) aqueous $NaHCO_3$; (iii) purification (vacuum distillation or column chromatography). The scale of the synthesis: [a] 100-500 mg; [b] 1-5 g; [c] 10-40 g of the isolated product. [d] With gaseous alkenes (products **1**-**3**, **31**-**39**), alkene component was taken in an excess. [e] *N,N-dimethylisobutyramide* was used as a starting material instead of *N*,*N*-dimethylacetamide (DMA). X-ray crystal structure of compounds **18**, **24**, **30,** and **41** are shown as thermal ellipsoids at 50% probability level; carbon – white, oxygen – red, nitrogen – blue, sulfur – yellow, bromine – orange, fluorine – green; hydrogen atoms are not shown.

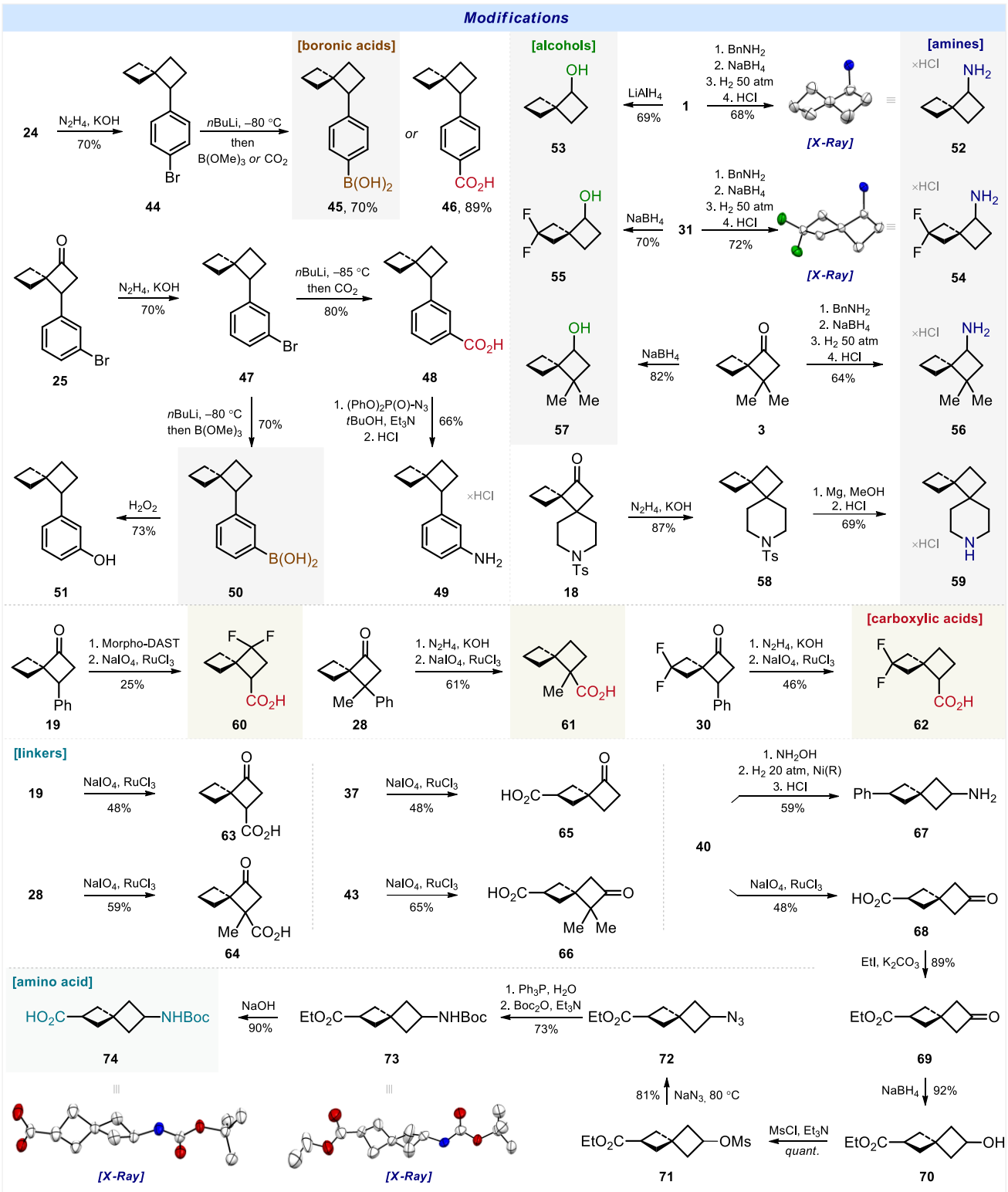

Scheme 3. Synthesis of functionalized spiro[3.3]heptanes for use as synthetic building blocks in medicinal chemistry. X-ray crystal structure of compounds **52**, **54**, **73**, and **74** (carbon – white, oxygen – red, nitrogen – blue, fluorine - green). Hydrogen and chlorine atoms are omitted for clarity. Ellipsoids are shown at a 50% probability level.

Despite the seeming simplicity of the current approach to spiro[3.3]heptanes, the preparation of only four products **1**,[18a] **3**,[16d] **37**,[18b] and **40**[16e] from Scheme 2 was previously reported in the literature by other methods.

Modifications. Representative modifications of the obtained ketones were undertaken to obtain various *mono*- and *bi*-functional spiro[3.3]heptanes for direct use in medicinal chemistry projects (Scheme 3).

The Wolff–Kishner reduction of ketone **24** gave bromide **44**. Treatment of the latter with *n*BuLi followed by the addition of either $B(OMe)_3$ or dry ice resulted in the formation of organoboron compound **45** or carboxylic acid **46**. The analogous tactic was applied to ketone **25** to obtain (via bromide **47**) carboxylic acid **48** and boronic acid **50**. The Curtius reaction of the latter gave aniline **49**. Oxidation of compound **50** with H_2O_2 gave phenol **51**.

Reductive amination of ketone **1** with benzylamine, followed by the subsequent *N*-Bn cleavage with H_2/Pd gave amine **52**. Reduction of ketone **1** with $LiAlH_4$ gave alcohol **53**. A similar strategy was used to synthesize amine **54** and alcohol **55** from ketone **31**; and amine **56** with alcohol **57** from ketone **3**. The Wolff–Kishner reduction of ketone **18** gave compound **58**. The *N*-Ts cleavage in the latter with magnesium powder in methanol gave amine **59** (Scheme 3). The structure of products **52** and **54** was confirmed by X-ray crystallographic analysis.[22]

The reaction of ketone **19** with morpho-DAST followed by oxidation of the phenyl ring with $NaIO_4$/$RuCl_3$ gave the fluorinated carboxylic acid **60**. The Wolff–Kishner reduction of ketone **28** followed by the oxidation of the phenyl ring gave carboxylic acid **61**. Analogously, from ketone **30**, the fluorinated carboxylic acid **62** was synthesized. Oxidation of the phenyl ring in ketone **19** with $NaIO_4$/$RuCl_3$ gave ketoacid **63**. Similarly, ketoacids **64**-**66**, **68** were synthesized from compounds **28**, **37**, **43**, and **40**, correspondingly. The reaction of ketone **40** with hydroxylamine followed by reduction of the intermediate oxime with Raney nickel gave amine **67** (Scheme 3).

Alkylation of carboxylic acid **68** with ethyl iodide gave ester **69**. Reduction of the carbonyl group in **69** with $NaBH_4$ gave alcohol **70**. *O*-Mesylation (via **71**) and the subsequent reaction with NaN_3 provided azide **72**. The Staudinger reduction of the azido group with PPh_3 followed by *N*-Boc protection gave compound **73**. Saponification of the ester group in **73** gave the *N*-Boc protected amino acid **74**.[23] The structure of products **73** and **74** was confirmed by X-ray crystallographic analysis.[22]

Incorporation into drugs. To validate the spiro[3.3]heptane scaffold as a saturated benzene bioisostere, we next aimed to incorporate this skeleton into a structure of existing drugs. We also planned to study the impact of such replacement on the experimental physicochemical properties and biological activity. We chose the FDA-approved anticancer drugs *Sonidegib*, *Vorinostat,* and the local anesthetic drug *Bupivacaine* with the *meta*-, *mono*- and *para*-substituted phenyl rings, correspondingly (Schemes 4-6).

<u>*Sonidegib*</u> (*meta*-substituted phenyl ring). Synthesis of saturated analogs of *Sonidegib* commenced from ketone **39** which was previously synthesized as a 3:1 mixture of two stereoisomers (Scheme 2). Separation of isomers *trans*-**39** and *cis*-**39** was undertaken by silica gel column chromatography. The stereoconfiguration of the obtained compounds was determined by 2D NMR spectroscopy. The reaction of the major isomer, *trans*-**39**, with tosyl isocyanide followed by acidic hydrolysis of the nitrile group gave carboxylic acid *trans*-**75**. Acylation of the corresponding heterocyclic amine gave racemic compound *trans*-**76** – a saturated analog of *Sonidegib.* Isomeric analog *cis*-**76** was obtained analogously from ketone *cis*-**39** via carboxylic acid *trans*-**75** (Scheme 4).

Next, we studied the impact of the replacement of the phenyl ring with spiro[3.3]heptane on the experimental physicochemical properties: water solubility, lipophilicity, and metabolic stability.

Replacement of the *meta*-substituted phenyl ring in *Sonidegib* by spiro[3.3]heptane (*trans*-**76**, *cis*-**76**) did not affect its water solubility. All three compounds were poorly soluble in water: ≤ 1 μM (Scheme 4).

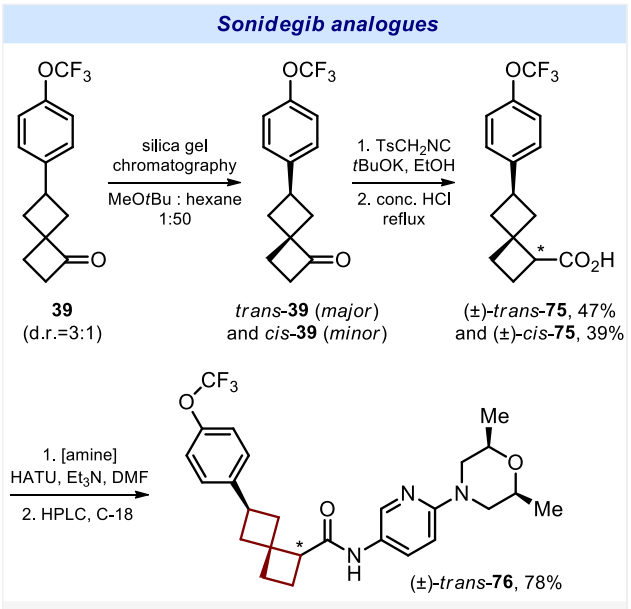

Compound	*Sol.*	*clogP*	*logD (7.4)*	$t_{1/2}$	CL_{int}	IC_{50}
Sonidegib	≤ 1	6.8	≥ 3.5	18	93	0.0015
(±)-*trans*-**76**	≤ 1	6.0	≥ 3.5	36	47	0.48
(±)-*cis*-**76**	≤ 1	6.0	≥ 3.5	156	11	0.24

Scheme 4. Synthesis and properties of *Sonidegib* analogs - compounds (±)-*trans*-**76** and (±)-*cis*-**76**. *Sol.* (μM): experimental kinetic solubility in phosphate-buffered saline, pH 7.4. *clogP*: calculated lipophilicity. *logD* (7.4): experimental distribution coefficient in *n*-octanol/phosphate-buffered saline, pH 7.4. CL_{int}, clearance intrinsic (μL/min/mg): experimental metabolic stability in human liver microsomes. $t_{1/2}$ (min): experimental half-time of a metabolic decomposition. IC_{50} (μM): experimental inhibition of Hedgehog signaling pathway by compounds in Gli reporter NIH3T3 cell line.

To estimate the influence of the replacement of the phenyl ring with spiro[3.3]heptane on lipophilicity, we used two parameters: calculated (clogP) [24] and experimental (logD) lipophilicities. Replacement of the phenyl ring with spiro[3.3]heptane decreased the lipophilicity by 0.8 units when examining clogP: 6.8 (*Sonidegib*) *vs* 6.0 (*trans*-**76**) vs 6.0 (*cis*-**76**) (Scheme 4). An impact on the experimental lipophilicity was not observed, as all three compounds had logD ≥ 3.5.

The effect of saturated bioisostere on metabolic stability was studied next. The incorporation of spiro[3.3]heptane into *Sonidegib* increased the metabolic stability in human liver

microsomes: CL_{int} (mg/(min•μL))=93 (*Sonidegib*) *vs* 47 (*trans*-**76**) *vs* 11 (*cis*-**76**). Moreover, incorporation of the spiro[3.3]heptane core into *Sonidegib* increased the life half time by 200-800% times: $t_{1/2}$ (min)=93 (*Sonidegib*) *vs* 47 (*trans*-**76**) vs 11 (*cis*-**76**).

Finally, we measured the experimental inhibition of the Hedgehog signaling pathway in cell-based Gli-Luc reporter NIH3T3 cell line by *Sonidegib*[25] versus its analogs *trans*-**76** and *cis*-**76** (for details see the Supporting Information, pages 271-272). In strict contrast to approved drugs, the use of racemic mixtures in primary biological testing in medicinal chemistry is common.[26] Therefore for the validation of the proof-of-concept,[27] we directly studied the biological activity of the available racemic compounds *trans*-**76** and *cis*-**76**.

On one hand, compounds *trans*-**76** and *cis*-**76** were found to be two orders of magnitude less active compared to the original drug *Sonidegib*: IC_{50} (μM) = 0.0015 (*Sonidegib*) *vs* 0.48 (*trans*-**76**) *vs* 0.24 (*cis*-**76**) (Scheme 4). On the other hand, both saturated analogs demonstrated a high level of micromolar inhibition (0.24-0.48 μM) of the Hedgehog signaling pathway in the Gli reporter NIH3T3 cell line.

Vorinostat (*mono*-substituted phenyl ring). From amine **52**, in three steps we synthesized a racemic compound **77** with the spiro[3.3]heptane core - a saturated analog of *Vorinostat* (Scheme 5). For comparison, we also obtained analog **78** (for details please see the Supporting Information, page 38). The structure of compound **78** was confirmed by X-ray crystallographic analysis.[22]

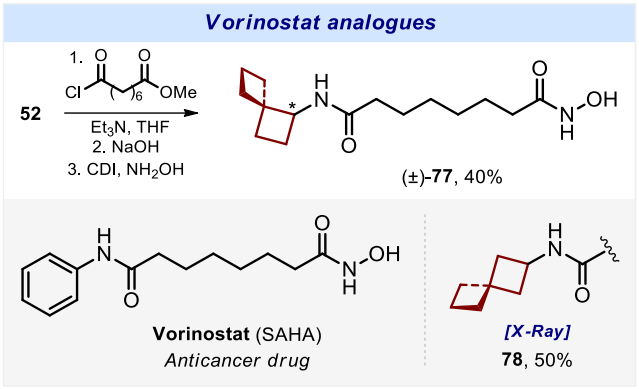

Scheme 5. Synthesis of *Vorinostat* analogs (±)-**77** and **78**.

To compare the biological activity of *Vorinostat* with its analogs **77** and **78**, we investigated their action on human hepatocellular carcinoma cells HepG2 by fluorescent confocal microscopy (Figure 1). The cells were incubated with the compounds for 48 h. Further staining with corresponding fluorescent dyes revealed that all three compounds promoted caspase-dependent cell death, and apoptosis (Figure 1, 2nd row), which subsequently culminated in necrosis – cellular death that is marked with compromised cellular membrane (Figure 1, 3rd row). *Vorinostat* treatment resulted in 7.2% and 12.2% of early apoptotic cells upon incubation for 48 hours at concentrations 5 μM and 50 μM respectively (Figure 2). Analogs **77** and **78** demonstrated similar efficacy only at 50 μM concentration (for details, please see the Supporting Information, page 273-276).

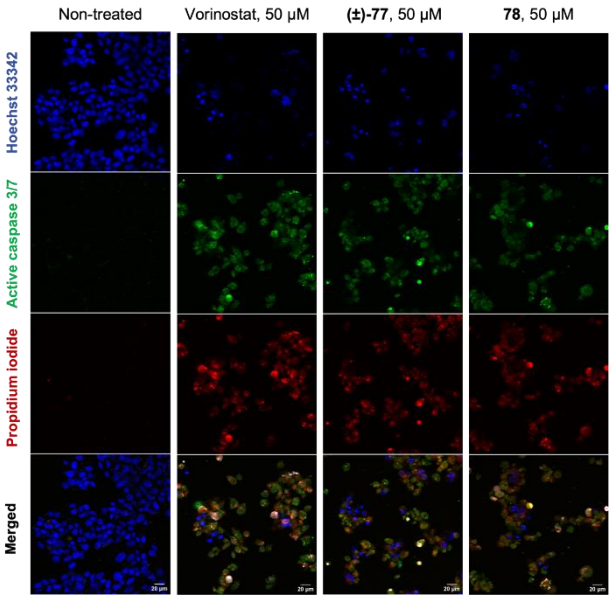

Figure 1. Fluorescent microscopy images of HepG2 cells treated with *Vorinostat* and analogs, (±)-**77** and **78**, at 50 μM during 48 h. First row: nuclei of cells are marked by Hoechst 33342 (blue). Second row: apoptotic cells are marked by CellEvent Caspase-3/7 Green Detection Reagent (green). Third row: necrotic cells are marked by propidium iodide (red). Fourth row: superposition of all three staining above.

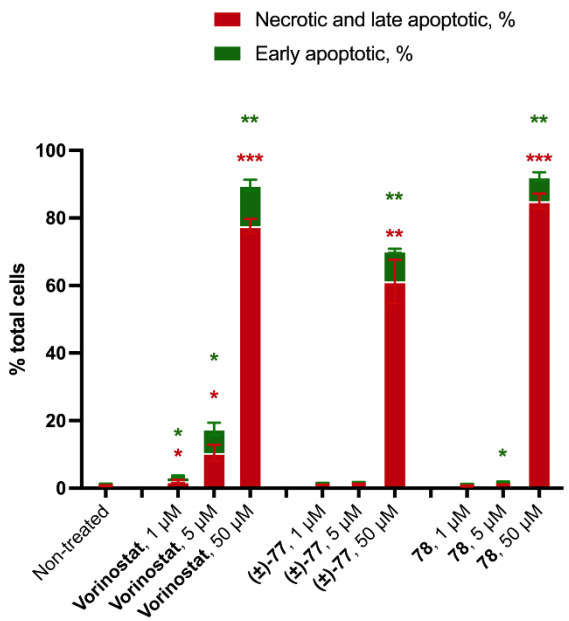

Figure 2. Death percentage of HepG2 cells after treatment with *Vorinostat* and analogs, (±)-**77** and **78** during 48 h. Red: necrotic cell death. Green: early apoptotic cell death. The data are presented as mean (n=3) ± SEM. * - indicates P < 0.05, ** - indicates P < 0.01, *** - P < 0.001 compared with the non-treated group.

The obtained results (Figures 1, 2) confirmed that *Vorinostat* and both its analogs **77**, **78** have similar cytotoxic and cytostatic activities in human cells.

Benzocaine (*para*-substituted phenyl ring). Compound **79**, a saturated analog of *Benzocaine*, was synthesized by acidic cleavage of the *N*-Boc group in ester **73** (Scheme 6). The product was obtained as a hydrochloride salt.

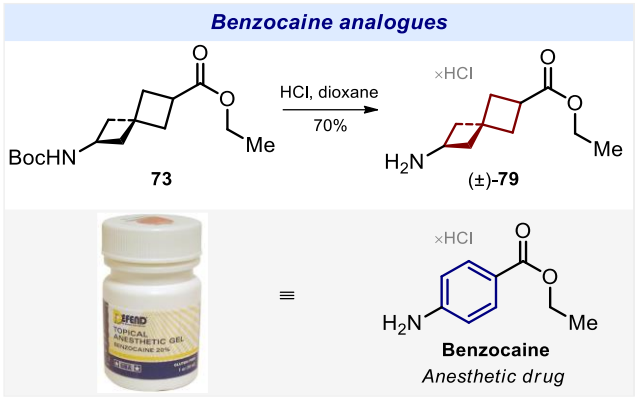

Scheme 6. Synthesis of benzocaine analog (±)-**79**.

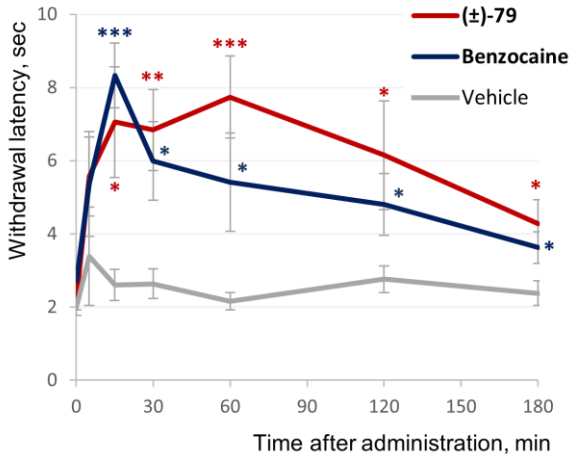

Figure 3. Time course of the antinociceptive effect of *Benzocaine* and its analog (±)-**79** in tail flick test on inbred mice. The data were presented as mean ± SEM. * - indicates P < 0.05; ** - indicates P < 0.01, and *** - indicates P < 0.001 compared with the vehicle-treated group.

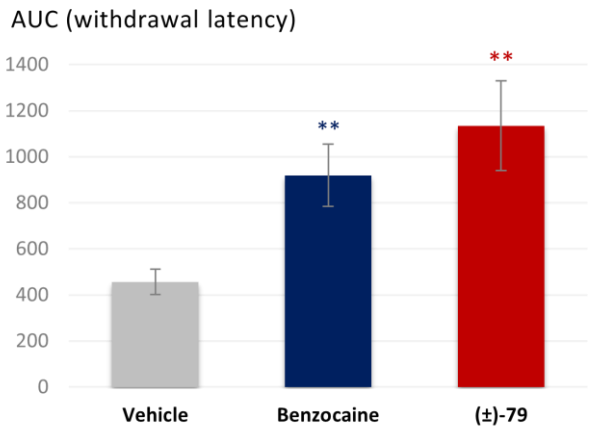

Figure 4. The area under the curve (AUC) of withdrawal latency of *Benzocaine* and its analog (±)-**79** in the tail flick test. The data were presented as mean ± SEM. ** - P < 0.01 compared with the vehicle-treated group.

We measured the experimental anesthetic activity of *Benzocaine* and its racemic analog **79** *in vivo*. We studied the antinociceptive effect of *Benzocaine* and compound **79** using the "tail flick test"[28] in 2-month-old CD-1 female mice (for details, see the Supporting Information, pages 277-279).[29] The results are presented in Figures 3 and 4.

Compound **79** demonstrated a significant antinociceptive activity compared to that of the vehicle (Figures 3, 4). Moreover, its activity was very similar to that of *Benzocaine* throughout the whole observation period (Figure 3). In addition, compound **79** showed a significant increase in coverage of analgesia time compared to that of the vehicle (Figure 4).

These biological experiments on *Sonidegib*, *Vorinostat*, *Benzocaine,* and their saturated analogs corroborated the original hypothesis that spiro[3.3]heptane is indeed a bioisostere of the phenyl ring.

Crystallographic analysis. To compare the geometric properties of spiro[3.3]heptanes and *para*-substituted phenyl ring, we used the exit vector plots tool. In this method, substituents at the disubstituted scaffold were simulated by two exit vectors n_1 and n_2 (Figure 5a). The relative spatial arrangement of vectors is described by four geometric parameters: the distance between *C*-atoms *r*, the plane angles φ_1 (between vectors n_1 and *C*-atom) and φ_2 (between n_2 and *C*-atom), and the dihedral angle θ defined by vectors n_1, *C*-*C* and n_2. An additional parameter - distance *d* between two carbon substituents (Figure 5a) - was also measured.

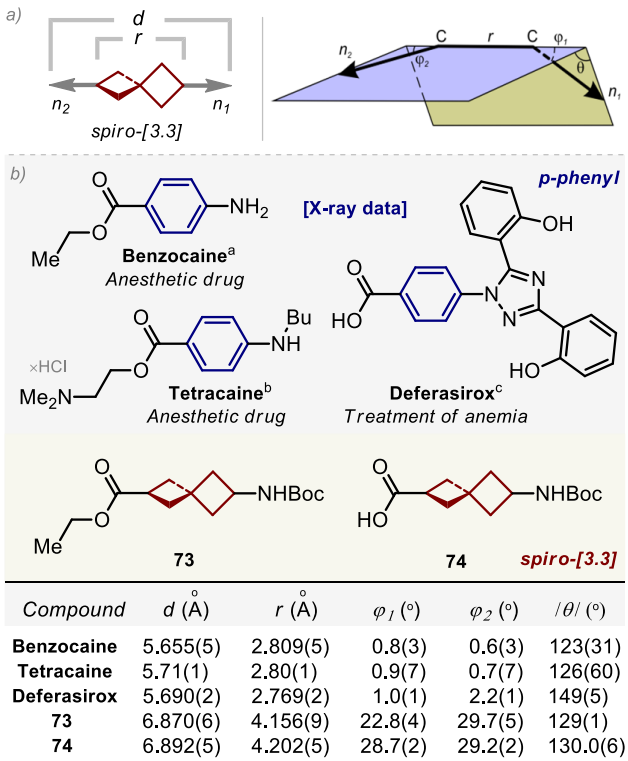

Compound	*d* (Å)	*r* (Å)	φ_1 (°)	φ_2 (°)	$\lvert\theta\rvert$ (°)
Benzocaine	5.655(5)	2.809(5)	0.8(3)	0.6(3)	123(31)
Tetracaine	5.71(1)	2.80(1)	0.9(7)	0.7(7)	126(60)
Deferasirox	5.690(2)	2.769(2)	1.0(1)	2.2(1)	149(5)
73	6.870(6)	4.156(9)	22.8(4)	29.7(5)	129(1)
74	6.892(5)	4.202(5)	28.7(2)	29.2(2)	130.0(6)

Figure 5. a) Definition of vectors n_1 and n_2, and geometric parameters *d*, *r*, φ_1, φ_2 and θ. Spiro[3.3]hexane is shown as an example. b) Geometric parameters *d*, *r*, φ_1, φ_2, and $|\theta|$ for *para*-substituted benzenes (*Benzocaine*, *Tetracaine*, *Deferazifox*), and saturated bioisosteres **73**, **74**. [a]Data is taken from ref. 30. [b]Data is taken from ref. 31. [c]Data is taken from ref. 32.

The values of *d*, *r*, φ_1, φ_2, and θ of spiro[3.3]heptanes were calculated from the X-ray data of compounds **73**, **74**. The corresponding parameters for *para*-substituted phenyl rings were calculated from the reported crystal data of three drugs – local anesthetics *Benzocaine*, [30] *Tetracaine,* [31] and the antianemic agent *Deferasirox* (Figure 5b). [32] Distance *r* in spiro[3.3]heptanes was ca. 1.4 Å longer than that in the *para*-

phenyl ring: 4.16-4.20 Å *vs* 2.77-2.81 Å (*para*-phenyl). The distance *d* between substituents in spiro[3.3]heptanes was also ca. 1.2 Å longer than that in the *para*-phenyl ring: 6.87-6.89 Å *vs* 5.66-5.71 Å (*para*-phenyl). Angles φ_1 and φ_2 in spiro[3.3]heptanes were 22.8-29.7°, whereby analogous angles in the *para*-phenyl ring were close to the ideal value of 0°: 0.6-2.2°. Spiro[3.3]heptanes were also non-planar: /θ/ = 129-130°. Interestingly, in the *para*-phenyl ring parameter /θ/ also deviated dramatically from the ideal value of 0°: 123-149°. However, parameter /θ/ alone is not representative, because the φ_1 and φ_2 angles are close to 0° (planar structure).

In general, vector characteristics of spiro[3.3]heptanes were different from those of the *para*-substituted phenyl ring. Spiro[3.3]heptanes have non-collinear exit vectors (φ_1, φ_2 = 22.8-29.7°), while the *para*-substituted phenyl ring – collinear ones (φ_1, φ_2 = 0.6-2.2°). Distance *d* in spiro[3.3]heptanes was ca. 1.2 Å longer than that in the *para*-phenyl ring. However, this difference in the angular model seems not to be dramatic, as supported by biological experiments on *Sonidegib*, *Vorinostat*, *Benzocaine* and their saturated analogs. In the known bioisoster bicyclo[1.1.1]pentane and the *para*-phenyl ring the distance *d* also differs by ca. 1.0 Å (Scheme 1).[3]

Summary. The phenyl ring is a key structural element in chemistry. It is the most popular ring in natural products,[1] bioactive compounds, and drugs.[2] During the past decade, scientists have developed saturated bioisosteres of the phenyl ring with collinear exit vectors: bicyclo[1.1.1]octane, cubane, bicyclo[2.2.2]octane, and 2-oxabicyclo[2.2.2]octane (Scheme 1). Here, we have synthesized, characterized, and validated spiro[3.3]heptane as a phenyl bioisostere with non-collinear vectors. Spiro[3.3]heptane was shown to mimic the *mono*-, *meta*- and *para*-substituted phenyl rings in drugs *Sonidegib*, *Vorinostat*, and *Benzocaine*, correspondingly.

We believe that this study opens up wide horizons in chemistry for making new/better analogs of any type of phenyl-containing molecules (medicinal chemistry, drug discovery, agrochemistry, polymer chemistry, supramolecular chemistry, *etc*).

Acknowledgments. This project has received funding from the European Research Council (ERC) under the European Union's Horizon 2020 research and innovation program (grant agreement No. 101000893 - BENOVELTY). PM is grateful to Dr. S. Shishkina (IOC, Kyiv) for the X-ray studies, to Dr. D. Bylina (Enamine) for HRMS measurements, Dr. Yuliia Holota (Bienta) for the help with physicochemical tests, Mrs Iryna Sadkova for proofreading the text, and to Dr. N. Meanwell (BMS) for the helpful discussions on the work.

Keywords: spiro[3.3]heptane • bicyclo[1.1.1]pentane • saturation • phenyl • bioisosteres

References

[1] Y. Chen, C. Rosenkranz, S. Hirte, J. Kirchmair. Ring systems in natural products: structural diversity, physicochemical properties, and coverage by synthetic compounds. *Nat. Prod. Rep.* **2022**, *39*, 1544-1556.

[2] (a) R. D. Taylor, M. MacCoss, A. D. G. Lawson. Rings in Drugs. *J. Med. Chem.* **2014**, *57*, 5845-5859. (b) J. Shearer, J. L. Castro, A. D. G. Lawson, M. MacCoss, R. D. Taylor. Rings in Clinical Trials and Drugs: Present and Future. *J. Med. Chem.* **2022**, *65*, 8699–8712.

[3] A. F. Stepan, C. Subramanyam, I. V. Efremov, J. K. Dutra, T. J. O`Sullivan, K. J. DiRico, W. S. McDonald, A. Won, P. H. Dorff, C. E. Nolan, S. L. Becker, L. R. Pustilnik, D. R. Riddell, G. W. Kauffman, B. L. Kormos, L. Zhang, Y. Lu, S. H. Capetta, M. E. Green, K. Karki, E. Sibley, K. P. Atchison, A. J. Hallgren, C. E. Oborski, A. E. Robshaw, B. Sneed, C. J. O`Donnell, Application of the Bicyclo[1.1.1]pentane Motif as a Nonclassical Phenyl Ring Bioisostere in the Design of a Potent and Orally Active γ-Secretase Inhibitor. *J. Med. Chem.* **2012**, *55*, 3414-3424.

[4] (a) N. D. Measom, K. D. Down, D. J. Hirst, C. Jamieson, E. S. Manas, V. K. Patel, D. O. Somers. Investigation of a Bicyclo[1.1.1]pentane as a Phenyl Replacement within an $LpPLA_2$ Inhibitor. *ACS Med. Chem. Lett.* **2017**, 8, 43-48. (b) Y. L. Goh, Y. T. Cui, V. Pendharkar, V. A. Adsool. Toward Resolving the Resveratrol Conundrum: Synthesis and *in Vivo* Pharmacokinetic Evaluation of BCP–Resveratrol. *ACS Med. Chem. Lett.* **2017**, *8*, 516-520. (c) Q. Pu, H. Zhang, L. Guo, M. Cheng, A. C. Doty, H. Ferguson, X. Fradera, C. A. Lesburg, M. A. McGowan, J. R. Miller, P. Geda, X. Song, K. Otte, N. Sciammetta, N. Solban, W. Yu, D. L. Sloman, H. Zhou, A. Lammens, L. Neumann, D. J. Bennett, A. Pasternak, Y. Han. Discovery of Potent and Orally Available Bicyclo[1.1.1]pentane-Derived Indoleamine-2,3-dioxygenase 1 (IDO1) Inhibitors. *ACS Med. Chem. Lett.* **2020**, *11*, 1548–1554.

[5] (a) B. A. Chalmers, H. Xing, S. Houston, C. Clark, S. Ghassabian, A. Kuo, B. Cao, A. Reitsma, C.-E. P. Murray, J. E. Stok, G. M. Boyle, C. J. Pierce, S. W. Littler, D. A. Winkler, P. V. Bernhardt, C. Pasay, J. J. De Voss, J. McCarthy, P. G. Parsons, M. T. Smith, H. M. Cooper, S. K. Nilsson, J. Tsanaktsidis, G. P. Savage, C. M. Williams. Validating Eaton's Hypothesis: Cubane as a Benzene Bioisostere. *Angew. Chem. Int. Ed.* **2016**, *55*, 3580-3585. (b) M. P. Wiesenfeldt, J. A. Rossi-Ashton, I. B. Perry, J. Diesel, O. L. Garry, F. Bartels, S. C. Coote, X. Ma, C. S. Yeung, D. J. Bennett, D. W. C. MacMillan. General access to cubanes as benzene bioisosteres. *Nature* **2023**, *618*, 513–518.

[6] (a) T. A. Reekie, C. M. Williams, L. M. Rendina, M. Kassiou. Cubanes in Medicinal Chemistry. *J. Med. Chem.* **2019**, *62*, 1078–1095. (b) S. S. R. Bernhard, G. M. Locke, S. Plunkett, A. Meindl, K. J. Flanagan, M. O. Senge. Cubane Cross-Coupling and Cubane–Porphyrin Arrays. *Chem. Eur. J.* **2018**, *24*, 1026-1030. (c) S. D. Houston, T. Fahrenhorst-Jones, H. Xing, B. A. Chalmers, M. L. Sykes, J. E. Stok, C. Farfan Soto, J. M. Burns, P. V. Bernhardt, J. J. De Voss, G. M. Boyle, M. T. Smith, J. Tsanaktsidis, G. P. Savage, V. M. Avery, C. M. Williams. The cubane paradigm in bioactive molecule discovery: further scope, limitations and the cyclooctatetraene complement. *Org. Biomol. Chem.* **2019**, *17*, 6790-6798. (d) K. J. Flanagan, S. S. R. Bernhard, S. Plunkett, M. O. Senge. Not Your Usual Bioisostere: Solid State Study of 3D Interactions in Cubanes. *Chem. Eur. J.* **2019**, *25*, 6941-6954. (e) J. Wlochal, R. D. M. Davies, J. Burton. Cubanes in Medicinal Chemistry: Synthesis of Functionalized Building Blocks. *Org. Lett.* **2014**, *16*, 4094-4097. (f) M. A. Dallaston, J. S. Brusnahan, C. Wall, C. M. Williams. Thermal and Sensitiveness Determination of Cubanes: Towards Cubane-Based Fuels for Infrared Countermeasures. *Chem. Eur. J.* **2019**, *25*, 8344-8352.

[7] (a) M. Zhong, E. Peng, N. Huang, Q. Huang, A. Huq, M. Lau, R. Colonno, L. Li. Discovery of functionalized bisimidazoles bearing cyclic aliphatic-phenyl motifs as HCV NS5A inhibitors. *Bioorg. Med. Chem. Lett.* **2014**, *24*, 5731-5737. (b) D. Bandak, O. Babii, R. Vasiuta, I. V. Komarov, P. K. Mykhailiuk. Design and Synthesis of Novel ^{19}F-Amino Acid: A Promising ^{19}F NMR Label for Peptide Studies. *Org. Lett.* **2015**, *17*, 226-229. (c) A. Aguilar, J. Lu, L. Liu, D. Du, D. Bernard, D. McEachern, S. Przybranowski, X. Li, R. Luo, B. Wen, D. Sun, H. Wang, J. Wen, G. Wang, Y. Zhai, M. Guo, D. Yang, S. Wang. Discovery of 4-((3′R,4′S,5′R)-6″-Chloro-4′-(3-chloro-2-fluorophenyl)-1′-ethyl-2″-oxodispiro[cyclohexane-1,2′-pyrrolidine-3′,3″-indoline]-5′-carboxamido)bicyclo[2.2.2]octane-1-carboxylic Acid (AA-115/APG-115): A Potent and Orally Active Murine Double Minute 2 (MDM2) Inhibitor in Clinical Development. *J. Med. Chem.* **2017**, *60*, 2819-2839.

[8] V. Levterov, Y. Panasyuk, K. Sahun, O. Stashkevich, V. Badlo, O. Shablykin, I. Sadkova, L. Bortnichuk, O. Klymenko-Ulianov, Y. Holota, J. Bas, P. Mykhailiuk. An "Ideal" Bioisoster of the para-substituted Phenyl Ring. *ChemRxiv* **2023** (doi: 10.26434/chemrxiv-2023-rbgz3).

[9] (a) P. K. Mykhailiuk. Saturated bioisosteres of benzene: where to go next? *Org. Biomol. Chem.* **2019**, *17*, 2839-2849. (b) G. M. Locke, S. S. R. Bernhard, M. O. Senge. Nonconjugated Hydrocarbons as Rigid-Linear Motifs: Isosteres for Material Sciences and Bioorganic and Medicinal Chemistry. *Chem. Eur. J.* **2019**, *25*, 4590-4647. (c) M. A. M. Subbaiah, N. A. Meanwell. Bioisosteres of the Phenyl Ring: Recent Strategic Applications in Lead Optimization and Drug Design. *J. Med. Chem.* **2021**, *64*, 14046–14128.

[10] For the common use of 3D-scaffolds in medicinal chemistry, see: (a) F. Lovering, J. Bikker, C. Humblet. Escape from Flatland: Increasing Saturation as an Approach to Improving Clinical Success. *J. Med. Chem.* **2009**, *52*, 6752-6756. (b) F. Lovering. Escape from Flatland 2: complexity and promiscuity. *Med. Chem. Commun.* **2013**, *4*, 515-519.

[11] More than 300 patents report the applications of spiro[3.3]heptanes in medicinal chemistry projects. The research was performed at Reaxys.db on 24.06.2023.

[12] We could find, however, two reports in the literature, where *poly*-substituted spiro[3.3]heptene (alkene) together with >20 other alkenes was used as potential replacement of *para*-substituted benzoic acid: (a) J. J. Swidorski, S. Jenkins, U. Hanumegowd, D. D. Parker, B. R. Beno, T. Protack, A. Ng, A. Gupta, Y. Shanmugam, I. B. Dicker, M. Krystal, N. A. Meanwell, A. Regueiro-Ren.

Design and exploration of C-3 benzoic acid bioisosteres and alkyl replacements in the context of GSK3532795 (BMS-955176) that exhibit broad spectrum HIV-1 maturation inhibition. *Bioorg. Med. Chem. Lett.* **2021**, *36*, 127823. (b) A. Regueiro-Ren, S.-Y. Sit, Y. Chen, J. Chen, J. J. Swidorski, Z. Liu, B. L. Venables, N. Sin, R. A. Hartz, T. Protack, Z. Lin, S. Zhang, Z. Li, D.-R. Wu, P. Li, J. Kempson, X. Hou, A. Gupta, R. Rampulla, A. Mathur, H. Park, A. Sarjeant, Y. Benitex, S. Rahematpura, D. Parker, T. Phillips, R. Haskell, S. Jenkins, K. S. Santone, M. Cockett, U. Hanumegowda, I. Dicker, N. A. Meanwell, M. Krystal. The Discovery of GSK3640254, a Next-Generation Inhibitor of HIV-1 Maturation. *J. Med. Chem.* **2022**, *65*, 11927–11948.

[13] Recently, spiro[3.3]heptane was also used as a potential replacement of the substituted toluene (R^1-C_6H_4-CH_2-R^2) moiety: Z. Cheng, Y. Wang, Y. Zhang, C. Zhang, M. Wang, W. Wang, J. He, Y. Wang, H. Zhang, Q. Zhang, C. Ding, D. Wu, L. Yang, M. Liu, W. Lu. Discovery of 2H-Indazole-3-carboxamide Derivatives as Novel Potent Prostanoid EP4 Receptor Antagonists for Colorectal Cancer Immunotherapy. *J. Med. Chem.* **2023**, *66*, 6218–6238.

[14] Reaction of cyclobutylketene to strained or activated alkenes: (a) L. Fitjer, U. Quabeck. Pentacyclo[11.3.0.01,5.05,9.09,13]hexadecane ([4.5]Coronane). *Angew. Chem. Int. Ed.* **1987**, *26*, 1023-1025. (b) L. Fitjer, C. Steeneck, S. Gaini-Rahimi, U. Schröder, K. Justus, P. Puder, M. Dittmer, C. Hassler, J. Weiser, M. Noltemeyer, M. Teichert. A New Rotane Family: Synthesis, Structure, Conformation, and Dynamics of [3.4]-, [4.4]-, [5.4]-, and [6.4]Rotane. *J. Am. Chem. Soc.* **1998**, *120*, 317-328. (c) S. V. Ryabukhin, K. I. Fominova, D. A. Sibgatulin, O. O. Grygorenko. Synthesis of three-dimensional fused and spirocyclic oxygen-containing cyclobutanone derivatives. *Tetrahedron Lett.* **2014**, *55*, 7240-7242. (d) W. Kong, Y. Zhou, Q. Song. Lewis-acid Promoted Chemoselective Condensation of 2-Aminobenzimidazoles or 3-Aminoindazoles with 3-Ethoxycyclobutanones to Construct Fused Nitrogen heterocycles. *Adv. Synth. Catal.* **2018**, *360*, 1943-1948.

[15] Addition of dichloroketene to alkenes: (a) L. Fitjer, A. Kanschik, M. Majewski. Synthesis and rearrangement of functionalized dispiro[3.0.3.3]undecanes – a new entry to [3.3.3]propellanes. *Tetrahedron Lett.* **1985**, *26*, 5277-5280. (b) L. Fitjer, A. Kanschik, M. Majewski. (±)-Modhephene and (±)-isocomene via cascade rearrangement. *Tetrahedron Lett.* **1988**, *29*, 5525-5528. (c) L. Fitjer, A. Kanschik, M. Majewski. Synthesis and rearrangement of dispiro[3.1.3.2]-, dispiro[3.0.3.3]- and dispiro[3.0.4.2]undecanes – new entries to [3.3.3]propellanes. *Tetrahedron* **1994**, *50*, 10867-10878. (d) L. Fitjer, M. Majewski, H. Monzó-Oltra. Synthesis of tricyclopentanoid sesquiterpenes via rearrangement routes: (±)-modhephene, (±)-epimodhephene and (±)-isocomene. *Tetrahedron* **1995**, *51*, 8835-8852. (e) M. Murakami, K. Takahashi, H. Amii, Y. Ito. Rhodium(I)-Catalyzed Successive Double Cleavage of Carbon-Carbon Bonds of Strained Spiro Cyclobutanones. *J. Am. Chem. Soc.* **1997**, *119*, 9307-9308. (f) L. Fitjer, R. Gerke, J. Weiser, G. Bunkoczi, J. E. Debreczeni. Helical primary structures of four-membered rings: (*M*)-trispiro[3.0.0.3.2.2]tridecane. *Tetrahedron* **2003**, *59*, 4443-4449.

[16] Some representative examples: (a) E. Buchta, K. Geibel. Spirocyclische Verbindungen, I. Spirane, Di-, Tri- und Tetraspirane. *Justus Liebigs Ann. Chem.* **1961**, *648*, 36-50. (b) E. Buchta, W. Theuer. Spirocyclische Verbindungen, II. 7-Oxa-spiro[3.5]nonan-2.2-Derivate, Oxa-oligospirane und Dioxo-dioxa-polyspirane. *Justus Liebigs Ann. Chem.* **1963**, *666*, 81-88. (c) E. Buchta, W. Merk. Oligo- und Polyspirane mit Cyclobutanringen ausgehend von Pentaerythrit-tetratosylat. *Naturwissenschaften* **1963**, *50*, 441. (d) E. Buchta, M. Fischer. Spirocyclische Verbindungen, VII. Spirane, Oligo- und Polyspirane mit Cycloheptan- und Cyclobutan-Ringen. *Chem. Ber.* **1966**, *99*, 1590-1517. (e) S. Knapp, T. G. M. Dhar, J. Albaneze, S. Gentemann, J. A. Potenza, D. Holten, H. J. Schugar. Photoinduced porphyrin-to-quinone electron transfer across oligospirocyclic spacers. *J. Am. Chem. Soc.* **1991**, *113*, 4010-4013. (f) G. R. Newkome, X. Lin, C. Yaxiong, G. H. Escamilla. Cascade polymer series. 27. Two-directional cascade polymer synthesis: effects of core variation. *J. Org. Chem.* **1993**, *58*, 3123-3129. (g) F. M. Menger, J. Ding. Spiro-Surfactants and -Phospholipids: Synthesis and Properties. *Angew. Chem. Int. Ed.* **1996**, *35*, 2137-2139. (h) N. Sakakibara, J. Igarashi, M. Takata, Y. Demizu, T. Misawa, M. Kurihara, R. Konishi, Y. Kato, T. Maruyama, I. Tsukamoto. Synthesis and Evaluation of Novel Carbocyclic Oxetanocin A (COA-Cl) Derivatives as Potential Tube Formation Agents. *Chem. Pharm. Bull.* **2015**, *63*, 701-709. (i) D. S. Radchenko, S. O. Pavlenko, O. O. Grygorenko, D. M. Volochnyuk, S. V. Shishkina, O. V. Shishkin, I. V. Komarov. Cyclobutane-Derived Diamines: Synthesis and Molecular Structure. *J. Org. Chem.* **2010**, *75*, 5941-5952. (j) A. Malashchuk, A. V. Chernykh, A. V. Dobrydnev, O. O. Grygorenko. Fluorine-Labelled Spiro[3.3]heptane-Derived Building Blocks: Is Single Fluorine the Best? *Eur. J. Org. Chem.* **2021**, 4897-4910.

[17] (a) B. M. Trost, D. E. Keeley, H. C. Arndt, M. J. Bogdanowicz. New synthetic reactions. Synthesis of cyclobutanes, cyclobutenes, and cyclobutanones. Applications in geminal alkylation. *J. Am. Chem. Soc.* **1977**, *99*, 3088-3100. (b) O. Sharon, A. A. Frimer. Synthesis and photosensitized oxygenation of cyclopropylidenecyclobutenes. *Tetrahedron* **2003**, *59*, 8153-8162. (c) A. A. Chernykh, D. S. Radchenko, O. O. Grygorenko, D. M. Volochnyuk, S. V. Shishkina, O. V. Shishkin, I. V. Komarov. Conformationally restricted glutamic acid analogues: stereoisomers of 1-aminospiro[3.3]heptane-1,6-dicarboxylic acid. *RSC Adv.* **2014**, *4*, 10894-10902. (d) M. G. Rosenberg, T. Schrievers, U. H. Brinker. Competitive 1,2-C Atom Shifts in the Strained Carbene Spiro[3.3]hept-1-ylidene Explained by Distinct Ring-Puckered Conformers. *J. Org. Chem.* **2016**, *81*, 12388-12400. (e) A. V. Chernykh, A. V. Chernykh, D. S. Radchenko, P. R. Chheda, E. B. Rusanov, O. O. Grygorenko, M. A. Spies, D. M. Volochnyuk, I. V. Komarov. *Org. Biomol. Chem.* **2022**, *20*, 3183-3200. (f) M. Jung, J. E. Muir, V. N. G. Lindsay. Expedient synthesis of spiro[3.3]heptan-1-ones via strain-relocating semipinacol rearrangements. *Tetrahedron* **2023**, *134*, 133296.

[18] (a) R. P. Robinson, B. J. Cronin, B. P. Jones. Tandem carbolithiation/cyclization of 2-(3-phenyl-2-propen-1-yl)oxazolines. A novel route to cyclobutane derivatives. *Tetrahedron Lett.* **1997**, *38*, 8479-8482. (b) A. B. Koldobskii, N. P. Tsvetkov, E. V. Solodova, P. V. Verteletskii, I. A. Godovikov, V. N. Kalinin. *Tetrahedron* **2010**, *66*, 3457-3462. (c) K. Kubota, E. Yamamoto, H. Ito. Copper(I)-Catalyzed Borylative exo-Cyclization of Alkenyl Halides Containing Unactivated Double Bond. *J. Am. Chem. Soc.* **2013**, *135*, 2635-2640. (d) M. L. Conner, M. K. Brown. Synthesis of 1,3-Substituted Cyclobutanes by Allenoate-Alkene [2+2] Cycloaddition. *J. Org. Chem.* **2016**, *81*, 8050-8060. (e) P. R. D. Murray, W. M. M. Bussink, G. H. M. Davies, F. W. van der Mei, A. H. Antropow, J. T. Edwards, L. A. D'Agostino, J. M. Ellis, L. G. Hamann, F. Romanov-Michailidis, R. R. Knowles. Intermolecular Crossed [2+2] Cycloaddition Promoted by Visible-Light Triplet Photosensitization: Expedient Access to

Polysubstituted 2-Oxaspiro[3.3]heptanes. *J. Am. Chem. Soc.* **2021**, *143*, 4055-4063. (f) H. O'Dowd, J. L. Manske, S. A. Freedman, J. E. Cochran. Ketoreductase-Catalyzed Access to Axially Chiral 2,6-Disubstituted Spiro[3.3]heptane Derivatives. *Org. Lett.* **2022**, *24*, 3431-3434. (g) L. Li, B. Matsuo, G. Levitre, E. J. McClain, E. A. Voight, E. A. Crane, G. A. Molander. Dearomative intermolecular [2+2] photocycloaddition for construction of C(sp^3)-rich heterospirocycles on-DNA. *Chem. Sci.* **2023**, *14*, 2713-2720.

[19] J.-B. Falmagne, J. Escudero, S. Taleb-Sahraoui, L. Ghosez. Cyclobutanone and Cyclobutenone Derivatives by Reaction of Tertiary Amides with Alkenes or Alkynes. *Angew. Chem. Int. Ed.* **1981**, *20*, 879-880.

[20] (a) A. Kolleth, A. Lumbroso, G. Tanriver, S. Catak, S. Sulzer-Mossé, A. De Mesmaeker. Synthesis of amino-cyclobutanes via [2 + 2] cycloadditions involving keteniminium intermediates. *Tetrahedron Lett.* **2016**, *57*, 2697–2702. (b) A. Kolleth, A. Lumbroso, G. Tanriver, S. Catak, S. Sulzer-Mossé, A. De Mesmaeker. *Tetrahedron Lett.* **2016**, *57*, 3510–3514. (c) A. Kolleth, A. Lumbroso, G. Tanriver, S. Catak, S. Sulzer-Mossé, A. De Mesmaeker. *Tetrahedron Lett.* **2017**, *58*, 2904–2909.

[21] D. Dagoneau, A. Kolleth, P. Quinodoz, B. Horoz, S. Catak, A. Lumbroso, S. Sulzer-Mossé, A. De Mesmaeker. Synthesis of Highly Substituted Cyclobutanones by a One-Pot Keteniminium-Enamine Process. *Helv. Chim. Acta* **2021**, *104*, e2100022.

[22] CCDC numbers: 2277176 (**18**), 2277177 (**24**), 2277178 (**30**), 2277179 (**41**), 2277180 (**52**), 2277181 (**54**), 2277182 (**73**), 2277183 (**74**), 2283954 (**78**).

[23] For previous preparations of compound **74**, see references 16i and 18f.

[24] clogP was calculated with "Cxcalc" (ChemAxon, version 22.5.0).

[25] S. Pan, X. Wu, J. Jiang, W. Gao, Y. Wan, D. Cheng, D. Han, J. Liu, N. P. Englund, Y. Wang, S. Peukert, K. Miller-Moslin, J. Yuan, R. Guo, M. Matsumoto, A. Vattay, Y. Jiang, J. Tsao, F. Sun, A. M. C. Pferdekamper, S. Dodd, T. Tuntland, W. Maniara, J. F. Kelleher, III, Y. Yao, M. Warmuth, J. Williams, M. Dorsch. Discovery of NVP-LDE225, a Potent and Selective Smoothened Antagonist. *ACS Med. Chem. Lett.* **2010**, *1*, 130–134.

[26] Because by testing a racemic mixture, one simultaneously tests two compounds (two enantiomers).

[27] Previously, the saturated scaffolds 2-oxabicyclo[2.1.1]hexane, bicyclo[3.1.1]heptane, [2]-ladderane, 3-azabicyclo[3.1.1]heptane and cuneanes were proposed to mimic the *meta*-substituted (hetero)aromatic rings in bioactive compounds. However, the biological validation of the corresponding saturated analogues has not been reported: (a) V. V. Levterov, Y. Panasyuk, V. O. Pivnytska, P. K. Mykhailiuk. Water-Soluble Non-Classical Benzene Mimetics. *Angew. Chem. Int. Ed.* **2020**, *59*, 7161-7167. (b) N. Frank, J. Nugent, B. R. Shire, H. D. Pickford, P. Rabe, A. J. Sterling, T. Zarganes-Tzitzikas, T. Grimes, A. L. Thompson, R. C. Smith, C. J. Schofield, P. E. Brennan, F. Duarte, E. A. Anderson. Synthesis of *meta*-substituted arene bioisosteres from [3.1.1]propellane. *Nature* **2022**, *611*, 721–726. (c) R. C. Epplin, S. Paul, L. Herter, C. Salome, E. N. Hancock, J. F. Larrow, E. W. Baum, D. R. Dunstan, C. Ginsburg-Moraff, T. C. Fessard, M. K. Brown. [2]-Ladderanes as isosteres for meta-substituted aromatic rings and rigidified cyclohexanes. *Nat. Commun.* **2022**, *13*, 6056. (d) D. Dibchak, M. Snisarenko, A. Mishuk, O. Shablykin, L. Bortnichuk, O. Klymenko-Ulianov, Y. Kheylik, I. V. Sadkova, H. S. Rzepa, P. K. Mykhailiuk. General Synthesis of 3-Azabicyclo[3.1.1]heptanes and Evaluation of Their Properties as Saturated Isosteres. *Angew. Chem. Int. Ed.* **2023**, e202304246. (e) E. Smith, K. D. Jones, L. O'Brien, S. P. Argent, C. Salome, Q. Lefebvre, A. Valery, M. Böcü, G. N. Newton, H. W. Lam. Silver(I)-Catalyzed Synthesis of Cuneanes from Cubanes and their Investigation as Isosteres. *J. Am. Chem. Soc.* **2023**, *asap* (doi.org/10.1021/jacs.3c03207).

[28] O. L. Davies, J. Raventós, A. L. Walpole A method for the evaluation of analgesic activity using rats. *Br. J. Pharmacol Chemother*. **1946**, 255-264.

[29] Study design, animal selection, handling and treatment were in accordance with Bienta Animal Care and Use Guidelines, and European Union directive 2010/63/EU.

[30] D. E. Lynch, I. McClenaghan. Monoclinic form of ethyl 4-amino-benzoate (benzocaine). *Acta Cryst.* **2002**, *E58*, o708-o709.

[31] H. Nowell, J. P. Attfield, J. C. Cole, P. J. Cox, K. Shankland, S. J. Maginn, W. D. S. Motherwell. Structure solution and refinement of tetracaine hydrochloride from X-ray powder diffraction data. *New J. Chem.* **2002**, *26*, 469-472.

[32] Q. Du, X. Xiong, Z. Suo, P. Tang, J. He, X. Zeng, Q. Hou, H. Li. Investigation of the solid forms of deferasirox: solvate, co-crystal, and amorphous form. *RSC Adv.* **2017**, *7*, 43151–43160.

Abstract

Spiro[3.3]heptane as a Non-collinear Benzene Bioisostere

Kateryna Prysiazhniuk,[a] Oleksandr P. Datsenko,[a] Oleksandr Polishchuk,[a] Stanislav Shulha,[a] Oleh Shablykin,[a,b] Liza Nikandrova,[c] Kateryna Horbatok,[c] Iryna Bodenchuk,[c] Petro Borysko,[c] Dmytro Shepilov,[c] Iryna Pishel,[c] Vladimir Kubyshkin,[a] Pavel K. Mykhailiuk[a]*

[a] Enamine Ltd., Winston Churchill Street78, 02094 Kyiv (Ukraine). Homepage: www.mykhailiukchem.org, www.enamine.net E-mail: Pavel.Mykhailiuk@gmail.com

[b] V.P. Kukhar Institute of Bioorganic Chemistry and Petrochemistry NAS of Ukraine, 02094 Kyiv (Ukraine).

[c] Bienta, Winston Churchill Street 78, 02094 Kyiv (Ukraine).

Spiro[3.3]heptane can mimic the *mono*-, *meta*- and *para*-substituted phenyl rings in drugs.